Fault diagnosis in district heating networks

Fault diagnosis in district heating networks

H Bahlawan[1], A Gambarotta[2,3], E Losi[1], L Manservigi[1*],

M Morini[2,3], C Saletti[3], P R Spina[1] and M Venturini[1]

[1] Dipartimento di Ingegneria, Università degli Studi di Ferrara, via Saragat 1, Ferrara 44122, Italy
[2] Centro Interdipartimentale per l'Energia e l'Ambiente (CIDEA), Università di Parma, Parco Area delle Scienze 181/a, Parma 43124, Italy
[3] Dipartimento di Ingegneria e Architettura, Università di Parma, Parco Area delle Scienze 181/a, Parma 43124, Italy

Abstract. District Heating Networks (DHNs), which dispatch thermal energy from a heat source to end-users by means of a heat carrier, are composed of pipes that can be affected by faults that endanger system reliability. Thus, reliable diagnostic approaches have to be employed to evaluate the health state of the DHN.
In the framework of the ENERGYNIUS research project, the authors of this paper developed a diagnostic approach aimed at detecting and identifying the most frequent faults that affect DHN pipes, i.e., water leakages, heat losses and pressure losses. The diagnostic approach detects and identifies pipe faults by coupling a DHN model with an optimization algorithm. As a result, the health indices of each pipe of the DHN, the fault position, its type and magnitude are provided.
This study investigates the capability of the diagnostic approach by using two datasets, in which challenging faults were hypothetically implanted in the DHN of the campus of the University of Parma.
The diagnostic approach successfully detected and identified both faults, by also accurately assessing fault magnitude. In addition, the relative error with which each DHN variable is predicted is lower than 0.06 %.

1. Introduction

Energy systems are experiencing a transition towards new design and management concepts in which energy networks (e.g., heat, electricity, gas, transport) will be integrated with each other to create the so-called smart energy systems.

This goal can be addressed by increasing the exploitation of renewable energy sources, optimizing national grids and pushing self-consumption strategies (e.g., energy districts). As a result, environmental, economic and social benefits are expected.

Due to the relevance of the topic, the authors developed several studies (e.g., [1-6]) and took part in research projects to promote the development of efficient smart energy systems. Among them, the current paper deals with the ENERGYNIUS project [7], (namely, ENERGY Networks Integration for Urban Systems) that was focused on the development of (i) strategies for integrating prosumers within energy districts that contribute to the regional and national energy networks, (ii) mathematical models for the real-time simulation of integrated energy networks, and (iii) methodologies for the optimized management, control and diagnosis of energy systems.

In a smart energy system, District Heating Networks (DHNs) clearly represent a key component employed to dispatch thermal energy from a heat source to end-users.

* Email address: lucrezia.manservigi@unife.it

As outlined in [8] and [9], the efficiency of DHNs depends on pipe health state, which can be compromised by three fault types, i.e., leakages, anomalous heat and pressure losses. Water leakages are caused by pipe corrosion [10] and failures in welded joints. Anomalous heat losses usually occur because of damages to the insulation and pipe casing ([10] and [11]). Finally, anomalous pressure losses are usually caused by the variation of pipe characteristics (e.g., roughness and diameter).

Thus, efficient diagnostic approaches are required to evaluate the comprehensive health state of the DHN, by detecting and identifying the faulty pipes. The detection task consists of localizing the faulty pipe, while the fault identification consists of identifying the fault type and estimating its magnitude.

In the literature, only a few diagnostic methodologies tackled this goal, by simultaneously detecting water leakages along pipes, and anomalous heat and pressure losses. This purpose has been recently pursued by Manservigi et al. [8] and Bahlawan et al. [9], who developed a novel diagnostic approach for detecting and identifying faults affecting DHN pipes. In [8] and [9], the DHN diagnosis was performed by coupling a DHN simulation model with an optimization algorithm. The DHN simulation model calculated the DHN variables, i.e., mass flow rate, temperature and pressure at each pipe and node of the DHN, while the optimization algorithm identified pipe health indices in such a manner that the error between measurement and simulated variables was minimized.

In addition, Manservigi et al. [8] investigated the effect of different fault magnitudes on the DHN variables. Subsequently, the diagnostic methodology was challenged at detecting and identifying faults affecting the DHN of the campus of the University of Parma. To this purpose, twenty-three datasets were generated by a digital twin of the DHN under analysis, in which different fault causes and magnitudes were implanted. As discussed in [9], the diagnostic approach correctly detected all datasets. In particular, Bahlawan et al. [9] focused on the diagnosis of eight out of twenty-three datasets, i.e., one healthy dataset and seven faulty datasets. In [9], the diagnostic approach detected and identified all faults, by also evaluating the correct health index of each pipe of the DHN. In addition, the DHN diagnosis was always physically sound, by always detecting and identifying the faulty zone.

These positive results were also strengthened by the fact that the relative error of each predicted DHN variable was in the range from - 0.06 % to 0.03 %.

In the current paper, the diagnostic approach developed and validated in [8] and [9] is further tested by means of two additional case studies simulated by means of the digital twin [9]. In the first dataset considered in this paper, one pipe is affected by anomalous pressure losses due to two simultaneous fault causes, i.e., increase in pipe roughness and decrease in pipe internal diameter. Instead, in the second dataset, two pipes are faulty due to the increase in the insulation thermal conductivity. The analyses reported in the current study are aimed at thoroughly evaluating the capability of the diagnostic approach, even in the most challenging scenarios.

The paper is structured as follows. First, the basics of the diagnostic approach are briefly reported. Second, the case study is described, by focusing on the DHN of the campus of the University of Parma, the simulation of the faulty datasets and their features. Then, the diagnostic approach is tested in the Results Section and finally conclusions are drawn.

2. Diagnostic approach

The diagnostic approach is aimed at detecting and identifying three fault types that affect the health state of DHNs, i.e., water leakages along pipes, anomalous pressure losses and thermal energy dissipations.

To evaluate the health state of the DHN, each pipe of the DHN is labelled by means of the three health indices, namely x_{Q}, x_{Rp} and x_{Rth}, which evaluate the occurrence of water leakages, anomalous pressure losses and anomalous heat losses, respectively. The health indices are equal to one under healthy conditions, while they are lower than one when a fault occurs; the lower the health index, the higher the magnitude of the fault.

To perform the diagnosis of the system, the diagnostic approach (see figure 1) exploits a DHN model that calculates the DHN variables, i.e., mass flow rate, temperature and pressure, of the DHN, by using balance equations under steady-state conditions.

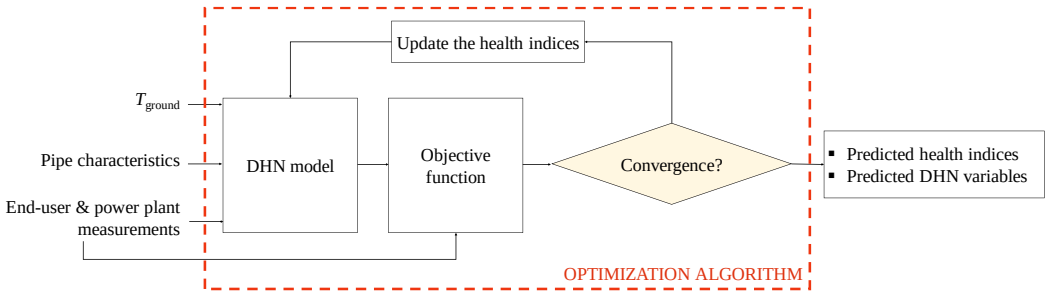

Figure 1. Scheme of the diagnostic approach.

The DHN health state is evaluated by using an optimization algorithm that adjusts the health indices of each pipe until the error function converges to a minimum. Further details about the diagnostic approach are reported in [8] and [9].

2.1. DHN model

The DHN model calculates the flow rate (Q) of each pipe, and the temperature (T) and pressure (p) at each node.

The mass flow rate Q that flows through each pipe is calculated by solving the mass flow rate balance at each node of the DHN, as in equation (1),

$$\sum x_{\mathrm{Q}} Q_{\mathrm{in}} - \sum Q_{\mathrm{EU}} - \sum Q_{\mathrm{out}} = 0 \tag{1}$$

where $x_{\mathrm{Q}} \cdot Q_{\mathrm{in}}$ is the mass flow rate that enters a node, Q_{EU} is the mass flow rate that leaves the node and flows towards an end-user, while Q_{out} is the mass flow rate that leaves the node and flows towards a split or a mixer.

The temperature of each node of the DHN is calculated by means of thermal power balances solved under steady-state conditions and by assuming that the specific heat c is constant. For each pipe of the DHN, the thermal power balance expressed in equation (2) includes three contributions: (i) the thermal power that enters a pipe, (ii) the thermal power that leaves the pipe, (iii) the thermal power losses due to water leakages and thermal dissipations through pipe walls.

$$cQT_{\mathrm{up}} - cx_{\mathrm{Q}}QT_{\mathrm{down}} - c\left(1 - x_{\mathrm{Q}}\right)Q\left(\frac{T_{\mathrm{up}} + T_{\mathrm{down}}}{2}\right) - \frac{1}{R_{\mathrm{th}}}\left(\frac{T_{\mathrm{up}} + T_{\mathrm{down}}}{2} - T_{\mathrm{g}}\right) = 0 \tag{2}$$

The thermal dissipations depend on the thermal resistance R_{th} (equation (3)), which accounts for internal convection and conduction of each pipe layer, i.e., steel pipe, insulation and external casing.

$$R_{\mathrm{th}} = x_{\mathrm{Rth}}\left[\frac{1}{\pi L D_{\mathrm{int,p}} k_{\mathrm{conv,int}}} + \frac{1}{2\pi L \lambda_{\mathrm{p}}}\ln\left(\frac{D_{\mathrm{ext}}}{D_{\mathrm{int}}}\right) + \frac{1}{2\pi L \lambda_{\mathrm{ins}}}\ln\left(\frac{D_{\mathrm{ins}}}{D_{\mathrm{ext}}}\right) + \frac{1}{2\pi L \lambda_{\mathrm{c}}}\ln\left(\frac{D_{\mathrm{c}}}{D_{\mathrm{ins}}}\right)\right] \tag{3}$$

The pressure of each node of the DHN is calculated by solving a set of equations as the one reported in equation (4), where p_{up} and p_{down} are the pressure of the upstream and downstream nodes, respectively, of each considered pipe.

$$-p_{\mathrm{up}} + p_{\mathrm{down}} + \Delta p = 0 \tag{4}$$

Pressure loss through a pipe, i.e., Δp, is calculated as in equation (5):

$$\Delta p = R_{\mathrm{p}} Q^2 \tag{5}$$

, where the coefficient R_p includes both concentrated and distributed pressure losses (see equation (6)):

$$R_p = \frac{1}{x_{Rp}}\left[\frac{8}{\rho(\bar{T})\pi^2 D_{int}^4}\left(f(\bar{T})\frac{L}{D_{int}}+\beta\right)\right] \quad (6)$$

2.2. Inputs, outputs and objective function

The diagnostic approach is fed by two types of input variables, i.e., independent and dependent variables.

The independent variables comprise the ground temperature, pipe characteristics, e.g., L, some measured end-user and power plant variables (see table 1).

Table 1. Inputs of the diagnostic approach.

		Variables	
Independent variables	Ground temperature	T_g	
	Pipe characteristics	L_i, $D_{int,P,i}$, $D_{ext,P,i}$, $D_{ins,i}$, $D_{c,i}$, β_i, $\lambda_{P,i}$, $\lambda_{ins,i}$, $\lambda_{c,i}$, ε_i	i = 1, …, N_P
	End-user measurements	$Q_{EU,i}^{meas}$, $\Delta T_{EU,i}$	i = 1, …, N_{EU}
	Power plant measurements	$T_{PP,i,s}^{meas}$, $p_{PP,i,s}^{meas}$, $p_{PP,i,r}^{meas}$	i = 1, …, N_{PP}
Dependent variables	End-user measurements	$T_{EU,i,s}^{meas}$, $T_{EU,i,r}^{meas}$, $p_{EU,i,s}^{meas}$, $p_{EU,i,r}^{meas}$	i = 1, …, N_{EU}
	Power plant measurements	$Q_{PP,i,s}^{meas}$, $Q_{PP,i,r}^{meas}$, $T_{PP,i,r}^{meas}$	i = 1, …, N_{PP}

Additional end-user and power plant measured variables (see once again table 1) are used as dependent variables, since they feed the objective function F_{ob} reported in equation (7), which compares the measured and predicted, i.e., calculated by the DHN model, variables.

The outputs of the diagnostic approach are the predicted health indices and the predicted DHN variables (figure 1 and table 2). For each pipe of the DHN, the diagnostic approach provides six health indices, i.e., $x_{Q,s}$, $x_{Rth,s}$, $x_{Rp,s}$, $x_{Q,r}$, $x_{Rth,r}$, $x_{Rp,r}$, which comprehensively assess the health state of both the supply and return pipelines. The predicted DHN variables are the mass flow rate Q that flows through each pipe, and pressure p and temperature T at each node of the DHN.

An optimization algorithm is used for minimizing the difference between the measured and predicted DHN variables of the objective function F_{ob} (equation (7)). To this purpose, the optimization algorithm adjusts the health indices until F_{ob} converges to a minimum, thus allowing the identification of the outputs of the diagnostic approach.

$$F_{ob} = A + B + C$$

$$A = \left(\frac{Q_{PP}^{meas}-Q_{PP}}{Q_{PP}^{meas}}\right)_s^2 + \left(\frac{Q_{PP}^{meas}-Q_{PP}}{Q_{PP}^{meas}}\right)_r^2$$

$$B = \left(\frac{T_{PP}^{meas}-T_{PP}}{T_{PP}^{meas}}\right)_r^2 + \sum_i^{N_{EU}}\left(\frac{T_{EU,i}^{meas}-T_{EU,i}}{T_{EU,i}^{meas}}\right)_s^2 + \left(\frac{T_{EU,i}^{meas}-T_{EU,i}}{T_{EU,i}^{meas}}\right)_r^2 \quad (7)$$

$$C = \sum_i^{N_{EU}}\left(\frac{p_{EU,i}^{meas}-p_{EU,i}}{p_{EU,i}^{meas}}\right)_s^2 + \left(\frac{p_{EU,i}^{meas}-p_{EU,i}}{p_{EU,i}^{meas}}\right)_r^2$$

Table 2. Outputs of the diagnostic approach.

	Variables	
Predicted health indices	$x_{Q,s,i}$, $x_{Q,r,i}$, $x_{Rp,s,i}$, $x_{Rp,r,i}$, $x_{Rth,s,i}$, $x_{Rth,r,i}$	i = 1, …, N_P
Predicted DHN variables	$Q_{s,i}$, $Q_{r,i}$	i = 1, …, N_P
	$T_{s,i}$, $T_{r,i}$, $p_{s,i}$, $p_{r,i}$	i = 1, …, N_n

3. Case study

3.1. District heating network

In this paper, the diagnostic approach is challenged at detecting and identifying faults that hypothetically affect the DHN of the campus of the University of Parma (figure 2), in Italy.

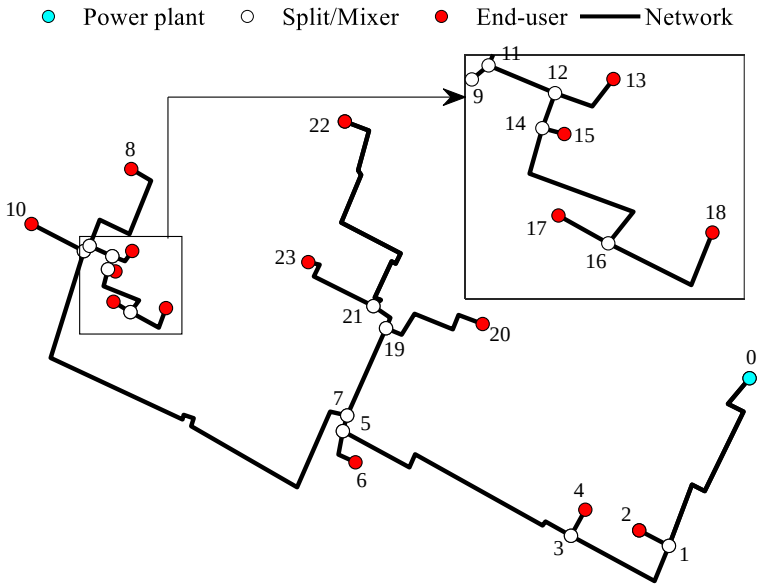

Figure 2. Scheme of the considered portion of the DHN of the campus of the University of Parma.

In the considered DHN, a thermal power plant heats the supply water, which is distributed by means of the supply pipeline towards twelve connected end-users i.e., departments, laboratories, classrooms and cafeterias [12]. The water mass flow rate enters the heat exchanger of each end-user and the return water goes back to the thermal power station.

The DHN includes both a supply and return pipeline, each one composed of twenty-three pipes and twenty-four nodes. As depicted in figure 2, each pipeline comprises one thermal power plant, twelve end-user nodes and eleven splitting and junction nodes.

In the case of the DHN of the campus of the University of Parma, the diagnostic model is required to predict one hundred thirty-eight health indices, since (i) each pipe is characterized by three health indices, (ii) each pipeline comprises twenty-three pipes and (iii) both the supply and the return pipelines are considered.

3.2. Digital twin of the DHN

In this paper, the DHN variables (Q, T and p) were generated by means of the simulation model developed in [13], which mimics the dynamic behaviour of the DHN investigated in this paper. Thus,

such model is used as a digital twin of the real DHN. Further details about model structure and equations are reported in [9] and [13].

3.3. Implanted faults

The pipelines of the DHN of the campus of the University of Parma are made of steel and are thermally insulated by means of a rock-wool layer and an external casing. Thus, under healthy conditions, the thermal conductivity values used in equation (3) are λ^*_P = 57 $W \cdot m^{-1} \cdot K^{-1}$, λ^*_{ins} = 0.04 $W \cdot m^{-1} \cdot K^{-1}$ and λ^*_c = 1 $W \cdot m^{-1} \cdot K^{-1}$. Pipe roughness ε^* is assumed equal to 0.1 mm.

The digital twin was used to generate the faulty datasets by modifying pipe characteristics, i.e., ε and λ_{ins}, D_{int}, as described in Bahlawan et al. [9].

The results presented in this paper focus on two faulty datasets, namely Fault #1 and #2 (see table 3), which are two challenging scenarios, since they comprise two simultaneous fault causes.

In this paper, each pipe of the DHN is labelled by using the upstream and downstream nodes.

Table 3. Implanted faults analyzed in this paper.

Fault no.	Effect of the fault	Faulty pipe	Fault location	Faulty parameter	Healthy parameter
#1	Anomalous pressure losses	19-20	Entire pipe	ε = 1.0 mm	ε^* = 0.1 mm
			10 % of pipe length	D_{int} = 37 mm	D^*_{int} = 100 mm
#2	Anomalous heat losses	12-14	Entire pipe	λ_{ins} = 0.40 $W \cdot m^{-1} \cdot K^{-1}$	λ^*_{ins} = 0.04 $W \cdot m^{-1} \cdot K^{-1}$
		19-20	Entire pipe	λ_{ins} = 2.00 $W \cdot m^{-1} \cdot K^{-1}$	

In Fault #1, pipe 19-20 is affected by anomalous pressure losses due to both the increase in pipe roughness and decrease in the pipe internal diameter (table 3). In the faulty dataset, the pipe roughness is one order of magnitude higher than the corresponding value considered in the healthy scenario along the entire pipe length, while the pipe internal diameter is 63 % lower than in the healthy scenario.

In Fault #2, two pipes are faulty, i.e., pipes 12-14 and 19-20, and anomalous heat losses are caused by an increase in λ_{ins} up to 2 $W \cdot m^{-1} \cdot K^{-1}$ along the entire length of the pipe.

4. Results

In this paper, the diagnosis of the DHN of the campus of the University of Parma was performed as follows:

- one steady-state time point was identified, since the diagnostic approach can only be employed under steady-state conditions. To this purpose, the ratio between the mean value and standard deviation of each DHN variable was calculated over sixty minutes. Such a ratio identifies a steady-state time point if its value is lower than 10^{-6} for each DHN variable;
- a gradient-based method (in this paper, the tool available in Matlab® environment [14] was employed), was used to obtain the health indices of each pipe. The starting values of the optimization were set equal to 1.0, while the search space was in the range from 10^{-3} (i.e., lower bound) and 1.0 (i.e., upper bound); such values correspond to 99.9 % decrease of health indices and the healthy condition, respectively. The optimization procedure stopped when the variation of the objective function was lower than 10^{-9}.

The diagnosis of the faulty datasets Fault #1 and #2 was conveyed by analyzing:

- the relative variation of each DHN variable, by comparing the faulty scenario, i.e., Y, to the healthy condition, i.e., Y^*, as in equation (8).

$$\delta Y = \frac{Y - Y^*}{Y^*} \quad , Y = Q, T, p \tag{8}$$

- the expected and predicted x_{Rp} and x_{Rth}, which are calculated by comparing R_{th} (calculated as in equation (3)) and R_p (calculated as in equation 6) of the faulty scenarios simulated by the digital twin to the same values under healthy condition [9];
- the expected and predicted R_{th} and R_p of the faulty pipe. In addition, the difference between the temperature and pressure under healthy condition (i.e., T^*, p^*) and the faulty scenario (i.e., T, p) are also provided;
- the absolute and relative error with which each DHN variable is evaluated [9];
- the heatmap charts, of which the colors highlight the predicted health indices. As discussed in [8], $x_{Rth,s}$ and $x_{Rth,r}$ predicted by the diagnostic approach are shown in a logarithmic scale. The actual faulty pipe and type are marked by means of the "X" symbol.

In this paper, the diagnostic approach is tested by means of simulated data that are fully reliable, since both feature and label noise do not occur. Instead, experimental data would have required the exploitation of data-cleaning approaches, as the ones documented in [15-18], in order to preliminarily assess data reliability.

4.1. Fault #1

As reported in table 3, the anomalous pressure losses affecting pipe 19-20 are caused by both an increase in the pipe roughness and decrease in the pipe internal diameter. As a result, both the mass flow rate and pressure at node 20 are lower than that of the healthy scenario (table 4). Such a fault mainly affects node 20 (see figure 3), since it is the downstream the node of the faulty pipe. Due to the fault, the health index $x_{Rp,s}$ is expected to be equal to 0.336 (table 4).

As can be grasped from table 4 and figure 4, the diagnostic approach correctly detects and identifies the faulty pipe and fault type, by also accurately predicting the health index magnitude. In fact, all health indices are found equal to 1, with the exception of the predicted $x_{Rp,s}$ of pipe 19-20, which is equal to 0.338. Based on this extremely positive result, the relative error of the predicted DHN variables is lower than 0.06 %.

Table 4. Fault #1: expected *vs.* predicted values.

	Expected value	Predicted value
Health index	$x_{Rp,s} = 0.336$	$x_{Rp,s} = 0.338$
R_p [kg^{-1}·m^{-1}]	645.51	643.53
Effect on the downstream node	$p_{20}^* - p_{20} = 9211.599$ Pa	$p_{20}^* - p_{20} = 9211.602$ Pa

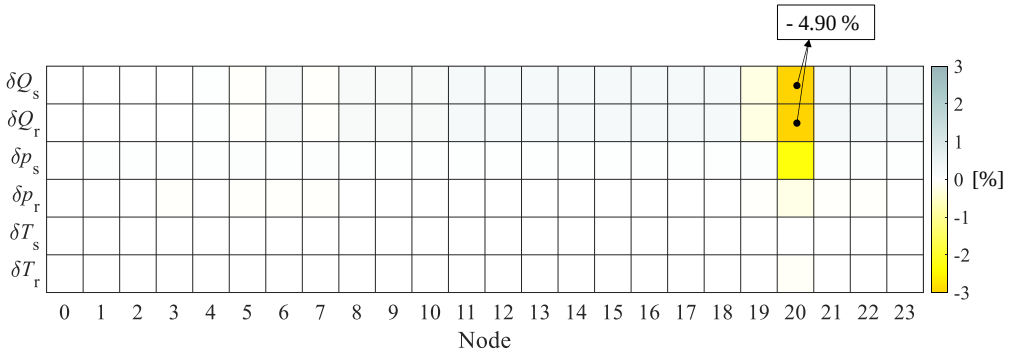

Figure 3. Comparison between Fault #1 and the healthy scenario.

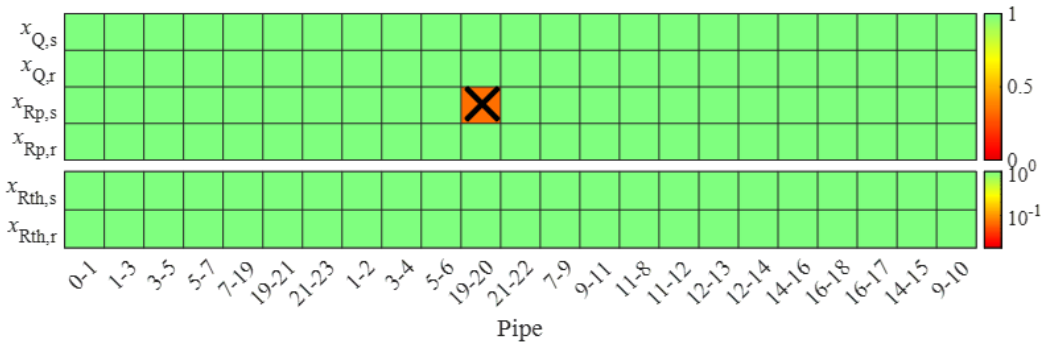

Figure 4. Predicted health indices for Fault #1.

4.2. Fault #2

Fault #2 affects two pipes, i.e., pipes 12-14 and 19-20, in which the thermal conductivity of the insulation material increases, as reported in table 3. Due to the fault, the temperature decrease in node 14 is as high as 1.94 °C with respect to the healthy scenario, while it is equal to 1.64 °C in node 20 (table 5).

Table 5. Fault #2: expected *vs.* predicted values.

	Pipe	Expected value	Predicted value
Health index	12 - 14	$x_{Rth,s} = 0.0205$	$x_{Rth,s} = 0.0213$
	19 - 20	$x_{Rth,s} = 0.1005$	$x_{Rth,s} = 0.1021$
$R_{th,}$ [K·W^{-1}]	12 - 14	0.000194	0.001934
$R_{th,}$ [K·W^{-1}]	19 - 20	0.00186	0.00184
Effect on the downstream node	12 - 14	$T^*_{14} - T_{14} = 1.9385$ °C	$T^* - T = 1.9371$ °C
	19 - 20	$T^*_{20} - T_{20} = 1.6421$ °C	$T^* - T = 1.6421$ °C

As can be grasped from figure 5, all nodes are affected by fault occurrence (though in a different degree), by exhibiting negative δT values, i.e., in the faulty scenario the temperature of each node is lower than that under healthy conditions. As expected, the temperature of the downstream nodes of the faulty pipes, i.e., nodes 14 through 18 and node 20, are mainly affected by the fault, since they exhibit the lowest δT values, i.e., -2.73 % and -2.31 %, respectively, while it is equal to -0.33 % in the remaining nodes at maximum.

Due to the fault magnitudes, the expected health index $x_{Rth,s}$ is equal to 0.02 and 0.100 in pipe 12-14 and 19-20, respectively, as shown in table 5. The diagnosis of the faulty dataset is reported in figure 6.

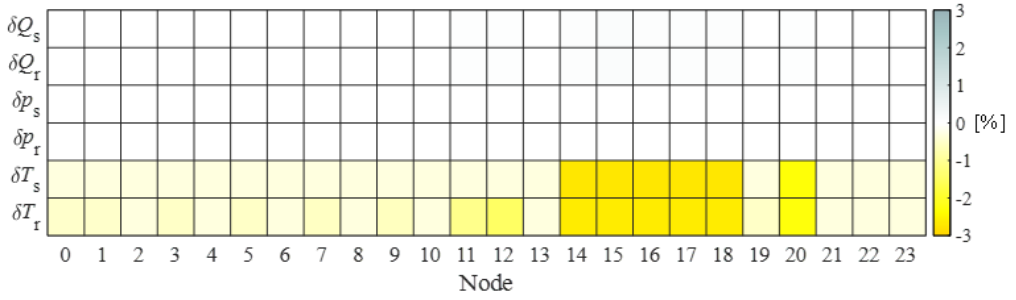

Figure 5. Comparison between Fault #2 and the healthy scenario.

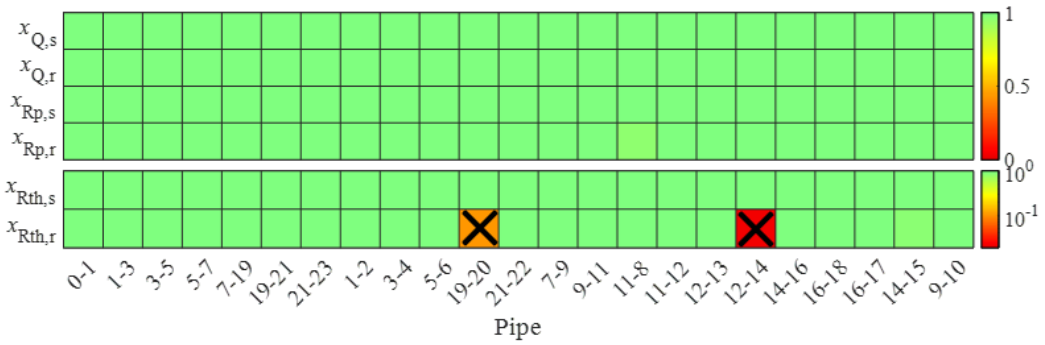

Figure 6. Predicted health indices for Fault #2.

Once again, the capability of the diagnostic approach is fully proved, since the faults are correctly detected, identified and evaluated. In fact, the lowest health indices are found in pipes 12-14 and 19-20, where the predicted $x_{Rth,s}$ values are equal to 0.0213 (pipe 12-14) and 0.1021 (pipe 19-20). In addition, no leakages and anomalous pressure losses are detected, since the predicted x_Q and x_{Rp} values are higher than 0.96 (figure 6).

Finally, the relative error with which the DHN variables are estimated is lower than 0.06 %.

5. Conclusions

In recent years, the concept of smart energy system has gained attention to move towards 100 % renewable energy systems, by pushing new design and management strategies for integrating multiple energy networks.

This goal has been recently investigated by the ENERGYNIUS (i.e., ENERGY Networks Integration for Urban Systems) research project, which focused on the role of prosumers and energy districts and developed mathematical models for real-time simulation of integrated multi-energy networks and their diagnosis.

In smart energy systems, District Heating Networks (DHNs) represent a key component employed to dispatch thermal energy from a heat source to end-users, by using a network composed of pipes. The reliability of a DHN clearly depends on the pipe health state, which can be compromised by three faults, i.e., water leakages, anomalous heat and pressure losses.

For this reason, reliable diagnostic approaches are required for detecting and identifying faults affecting the DHN pipes. To this purpose, the authors of this paper developed a novel diagnostic approach that is able to detect and identify the most common pipe failures under steady-state conditions. The diagnostic approach coupled a DHN model that calculated the DHN variables, i.e., mass flow rate, temperature and pressure, with an optimization algorithm. The outputs of diagnostic approach are the health indices of all pipes of the DHN.

In this paper, the diagnostic approach was applied to two challenging datasets in which different faults were implanted in the DHN of the campus of the University of Parma, whose variables were generated by means of a digital twin of the DHN.

In the first dataset, one pipe was faulty due to the simultaneous increase in pipe roughness and decrease in the pipe internal diameter. As a result, anomalous pressure losses occurred. In the second dataset, two faulty pipes were simulated, in which anomalous heat losses were caused by an increase in the insulation thermal conductivity.

The diagnostic approach successfully detected and identified the faults of both datasets, since the faulty pipe and fault type were found, by also accurately estimating the fault magnitude. The extremely positive result was also conveyed by the fact that the relative error with which the diagnostic approach calculated the DHN variable was always lower than 0.06 %.

Acknowledgements

This paper was carried out in the framework of the research program "ENERGYNIUS - ENERGY Networks Integration for Urban Systems (PG/2018/632084)".

References

[1] Manservigi L, Cattozzo M, Spina PR, Venturini M and Bahlawan H 2020 *Energies* **13** 1507
[2] Bahlawan H, Morini M, Pinelli M and Spina PR 2019 *Appl. Therm. Eng.* **160** pp. 1-11
[3] Bahlawan H, Losi E, Manservigi L, Morini M, Pinelli M, Spina PR and Venturini M 2020, "Optimal design and energy management of a renewable energy plant with seasonal energy storage", Atti, 100RES 2020 – Applied Energy Symposium (ICAE), Virtuale Online, Pisa, 25 – 30 Ottobre.
[4] Bahlawan H, Gambarotta A, Losi E, Manservigi L, Morini M, Spina PR and Venturini M 2021 *J Eng Gas Turbine Power* **143**, 061013
[5] Bahlawan H, Morini M, Pinelli M, Spina PR and Venturini M 2021 *Appl. Therm. Eng.* **187**, pp. 1-14
[6] Bahlawan H, Morini M, Pinelli M, Spina PR and Venturini M 2021 *Energy Convers. Manag.*, **249**, pp. 1-16
[7] https://www.energynius.it/home-page-it
[8] Manservigi L, Bahlawan H, Losi E, Morini M, Spina PR and Venturini M 2022 *Energy* **251** 123988
[9] Bahlawan H, Ferraro N, Gambarotta A, Losi E, Manservigi L, Morini M, Saletti C, Spina P R and Venturini M 2022 *Energy Convers. Manag.* **266** 115837
[10] Hallberg D, Stojanovic B and Akander J 2012 *Struct. Infrastruct. Eng* **8** 41-54
[11] Buffa S, Fouladfar MH, Franchini G, Gabarre IL and Chicote MA 2021 *Appl. Sci.* **11** 455
[12] Ancona MA, Branchini L, De Lorenzi A, De Pascale A, Gambarotta A, Melino F and Morini M 2019 *AIP Conference Proceedings* 2191 020009
[13] De Lorenzi A, Gambarotta A, Morini M, Rossi M and Saletti C 2020 *Energy* **205** 118054
[14] Matlab release 2020a: https://it.mathworks.com
[15] Losi E, Venturini M, Manservigi L, Ceschini GF and Bechini G 2019 *J. Eng. Gas Turbines Power* **141** 111019
[16] Manservigi L, Venturini M, Ceschini GF, Bechini G and Losi E 2020 *J. Eng. Gas Turbines Power* **142** 021009
[17] Manservigi L, Murray D, Artal de la Iglesia J, Ceschini GF, Bechini G, Losi E and Venturini M 2022 *ISA Trans.* **123** 323–338
[18] Manservigi L, Venturini M, Losi E, Bechini G and Artal de la Iglesia J 2022 *Machines* **10** 228